J. Enzyme Inhibition, 2000, Vol. 15, pp. 547–556
Reprints available directly from the publisher
Photocopying permitted by license only

INHIBITION OF AChE: STRUCTURE-ACTIVITY RELATIONSHIP AMONG CONFORMATIONAL TRANSITION OF Trp84 AND BIMOLECULAR RATE CONSTANT

C. BERTONATI[a], M. MARTA[a,b], M. PATAMIA[b], A. COLELLA[a] and M. POMPONI[a,*]

[a]*Istituto di Chimica e Chimica Clinica, Facoltà di Medicina, UCSC, Rome, Italy;* [b]*Centro Chimica dei Recettori del CNR, Rome, Italy*

(Received 20 January 2000)

In this study the authors attempt to correlate kinetic constants for carbamylation of AChE, by a series of carbamate inhibitors, with the conformational positioning of Trp84 in transition state complexes of the same carbamates with *Torpedo* AChE, as obtained by computerized molecular modelling. They present evidence for changes in the distance of the carbamates from the center of the indole ring which can be correlated with the bimolecular rate constants for inhibition. As a result the greater the distance from Trp84, the smaller the bimolecular inhibition constant value, k_i ($= k_2/K_a$), becomes. In conclusion, the value of the bimolecular rate constant for selected AChE inhibitors (structural changes that have been hypothesised or natural alkaloids of unknown activity) which possess similar size and rigidity, can be obtained. Under these conditions energy minimization alone seems to be sufficient even to accurately predict protein-substrate interactions that actually occur. Modelling studies also suggest that conformational re-orientation of Trp84 in the transition state could produce an overall movement of the Cys67-Cys94 loop.

Keywords: Acetylcholinesterase catalysis; Cholinesterase inhibition; Bimolecular rate constants; Conformations; Alzheimer's disease

* Corresponding author. E-mail: m.pomponi@uniserv.ccr.rm.cnr.it.

INTRODUCTION

Acetylcholinesterase (AChE, EC 3.1.1.7) hydrolyses the neurotransmitter acetylcholine (ACh), thereby terminating neurotransmission and allowing rapid and repetitive responses.

Notwithstanding the abundance of data collected on the extraordinary catalytic efficiency[1] of AChE ($k_{cat}/K_m \approx 1.4 \times 10^8\ M^{-1}s^{-1}$), comprehensive characterization of its structure-activity relations has only lately begun to emerge. This has been triggered by the elucidation of the three dimensional structure of *Torpedo californica* acetylcholinesterase (*Tc*AChE)[2] which shows that at the base of a narrow gorge about 20 Å in depth lies the catalytic triad: Ser200, Glu327 and His440.[3] Among the structural elements of this active site there is the Trp84 residue, the anionic subsite residue. The π-system of Trp84 is involved in dipole-dipole interactions with the charged substrate/inhibitor;[4] Trp84 is also part of that Ω surface loop (Cys67-Cys94) of AChE, which constitutes the thin portion of the gorge wall.[5] This loop is a structurally conserved element which, probably, plays a critical role in some sort of conformational adaptation fundamental for the molecular function.[6] Given the above situation, the questions being asked are: (a) is there any conformational re-orientation of Trp84 in the well-defined binding site of AChE? (b) would the conformational re-orientation of Trp84 produce structural modification of the loop shape?

With this aim the authors have examined the orientation of the Trp84 side chain after modelling simulation of the different degrees to which AChE is inhibited by using a series of long acting, centrally acting, reversible inhibitors (Figure 1, **2–9**), analogues of the alkaloid physostigmine. Acetylcholinesterase inhibitors (donepezil, tacrine, rivastigmine, metrifonate, physostigmine, huperzine A, ...) are the only FDA-approved primary treatment for patients with mild to moderately severe Alzheimer's disease.[7]

MATERIALS AND METHODS

The alkaloids (pyrrolo[2,3-b]indol-5-ol 3,3a,8,8a-hexahydro-1,3a,8-trimethyl-N-alkyl-carbamates, 3aS-cis) were prepared according to the procedure of the authors.[8] All the reagents for synthesis of the inhibitors were purchased from Aldrich Chemical Co. and were of analytical grade. We thank Professor Arnold Brossi and Prof. Nigel H. Greig (NIH, Bethesda) for providing physovenine, Dr. Yuhpyng L.Chen (Pfizer, Groton, CT) for providing 8-Carbaphysostigmine.

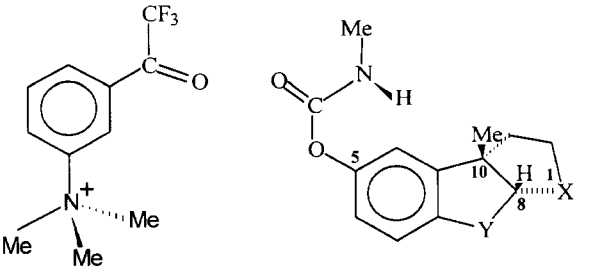

1 2-9

FIGURE 1 *Molecular formulas.* *m*-(N,N,N-trimethylammonio)-trifluoroacetophenone (TMTFA, **1**); 8-Carbaphysostigmine (**2**, Y = CH_2, X = NEt, R = CH_3); physostigmine (Phy, **3**, Y = NCH_3, X = NCH_3, R = CH_3); physovenine (**4**, Y = NCH_3, X = O, R = CH_3); heptyl-Phy (**5**, Y = NCH_3, X = NCH_3, R = C_7H_{15}); dimethyl-Phy (**6**, Y = NCH_3, X = NCH_3, the carbamic nitrogen is di-substituted: $N(CH_3)_2$); decyl-Phy (**7**, Y = NCH_3, X = NCH_3, R = $C_{10}H_{21}$); ethyl-Phy (**8**, Y = NCH_3, X = NCH_3, R = C_2H_5); propyl-Phy (**9**, Y = NCH_3, X = NCH_3, R = C_3H_7).

The identity of inhibitors was confirmed by spectroscopic methods. For nuclear magnetic resonance (NMR) spectra each compound was dissolved in $CDCl_3$. Trimethylsilane was included as an internal standard. The ^{1}H-(300 Mhz) and ^{13}C-NMR (75.5-Mhz) were obtained on a Varian Gemini spectrometer. Structures of the inhibitors used are shown in Figure 1.

The method of Ellman *et al.*[9] was employed to measure acetylthiocholine (ATC) hydrolysis. Adding the substrate to the medium containing AChE from Electrophorus electricus (Sigma Chemicals, Type V-S) in 0.1% bovine serum albumin and buffer started the reaction. When inhibition by carbamates was measured, the enzyme was added last, to prevent its carbamoylation in the absence of substrate. 5,5-Dithiobis(2-nitrobenzoic acid) (DTNB) was purchased from Sigma. The enzyme stock solutions (4 units/ml) were prepared in 0.10 M sodium phosphate buffer (pH 8.0). The assay medium contained 0.5 mM ATC iodide, 0.25 mM 5,5-dithiobis(2-nitrobenzoic acid), 0.1 M sodium phosphate, pH 8.0, and the reaction was monitored at 410 nm by means of graphics software (Varian Cary 3E) at 20 ° using thermostatted (Haake) cells. The Michaelis constant K_m (~0.10 mM at 25 °C) had been previously determined. Each experiment was repeated three times.

Inhibitors that have a carbamoyl moiety, such as physostigmine and its analogues, were slowly hydrolyzed by AChE according to the generalized scheme I.[10]

$$E + I \underset{k_{-1}}{\overset{k_1}{\rightleftharpoons}} E*I \xrightarrow{k_2} E*I' \xrightarrow{k_3} E + P$$

SCHEME 1 AChE kinetics.

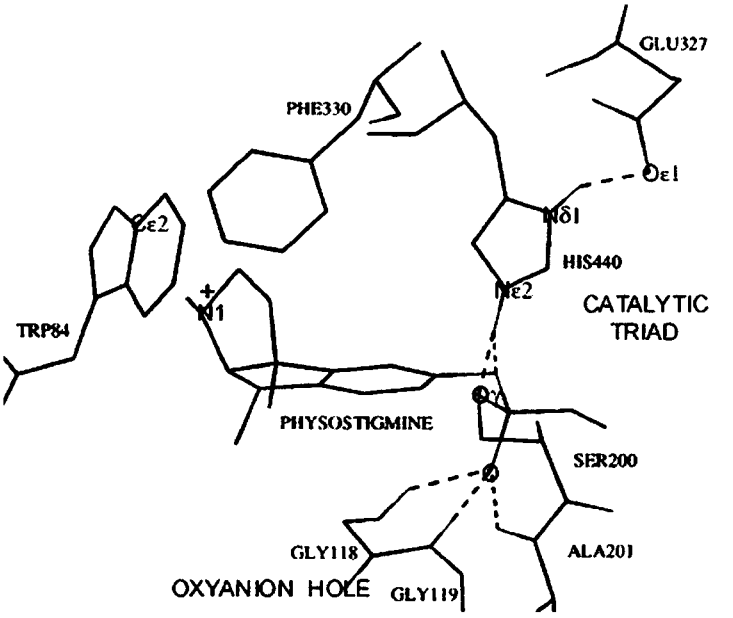

FIGURE 2 Closeup of the Phy-TcAChE complex showing its covalent bonding with Ser200. The amino acid side chains are shown as solid lines. The dashed lines denote hydrogen bonds to the putative residues in the oxyanion hole, i.e., Gly118, Gly119, and Ala201, and the catalytic triad, i.e., Ser200, His440, and Glu327. In addition to the triad, Trp84 is also shown. The solid line which marks the bond between the Ser200 Oγ and the carbonyl carbon of the inhibitor is the bond produced in the transition state.

In the first step, the inhibitor binds to the enzyme's active site in a non-covalent fashion to form an enzyme inhibitor complex E*I, then the enzyme starts its catalytic cycle, usually resulting in a rate determining carbamoylation of the residue Ser200. The covalent reaction intermediate mimics the normal covalent reaction intermediate occurring during catalysis; k_2 and k_3 are first-order rate constants of carbamoylation and reactivation, respectively. However the inhibiting activity of carbamates is mainly controlled by the bimolecular carbamylating rate constant k_i $(= k_2/K_a)$ where K_a is a Michaelis-type constant $(= (k_{-1} + k_2)/k_{+1})$. Equilibrium is approached

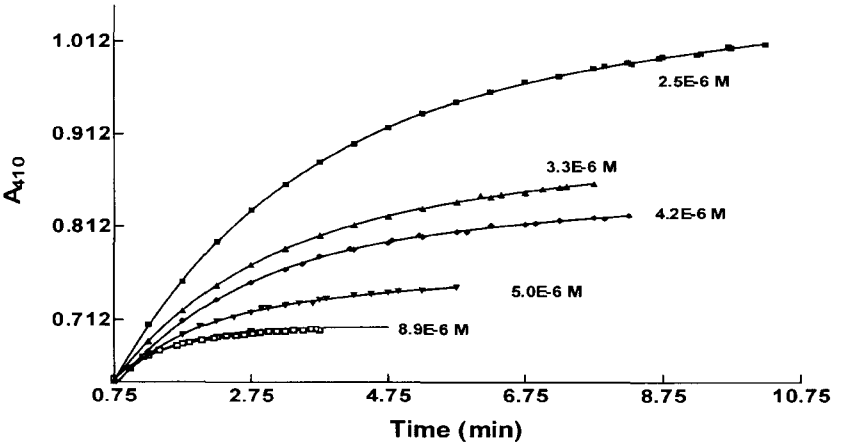

FIGURE 3 *Computer fitting of the progress curve.* Computer fitting by Marquardt's method[18] of the progress curve of eel AChE inhibition with different concentrations of physostigmine; substrate concentration $= 1.22 \times 10^{-1}$ M. Points are actual data values, and the lines are the graphical plots of the fitted polynomial equation. Inhibition at 20 °C. AChE activity was determined by a slight modification of the method used by Ellman *et al.*[9]

when $k_{-1} \gg k_2$ but there appears to be no *a priori* reason for k_{-1} to be greater than k_2, even if it is a very useful assumption. In the simultaneous presence of both the substrate and the inhibitor, the course product formation can be described by the fit of the exponential equation $[P] = D^*(k_3{*}t/(B + k_3) + (B/(B + k_3)^2)^*(1\text{-}\exp\text{-}((B + k_3)^*t)))$[10] where $B = k_2/A$; $A = 1 + K_a/[I] + (K_a{*}[S]_o)/(K_m{*}[I])$; $D = (k_3{*}K_a{*}[S]_o{*}[E]_o)/(A^*K_m{*}[I])$. The plot of the reciprocal of the inhibitor concentration against 1/B approximates a straight line in the range of concentrations used (Figure 4). In Figure 3 is reported the time course of substrate hydrolysis in the presence of inhibitor **3**. The ln of association constant (1/*K*i) for TMTFA (**1**) is 34.3[11]; ln k_i for **2** is 14.8 (range: 0.17–0.77 μM); for **3** is 14.7 (range: 2.8–9.4 μM); for **4** is 13.3 (range: 0.6–6.9 μM); for **5** is 12.8 (range 5.0–20 μM); for **6** is 12.5 (range 7.0–28.0 μM); for **7** is 12.0 (range: 20–50 μM); for **8** is 13.2 (range 3.1–10.2 μM); for **9** is 11.9 (range 13.1–20.1 μM).

The crystallographic coordinates of the *Tc*AChE complex with the transition state analogue inhibitor *m*-(N,N,N-trimethylammonio)-2,2,2-trifluoroacetophenone, TMTFA, were used as a basis for the modelling procedures (Brookhaven Protein Data, ID Codes 1AMN). Silicon Graphics workstation Indigo2 using the 6.4 version of SYBYL, (program from Tripos Associated Inc., St. Louis, Missouri), was used. Physostigmine, or one of its analogues, was manually placed in the catalytic site of AChE by

manual docking using the X-ray coordinates of TMTFA-AChE complex as template. Creating a subset of AChE minimized the different complexes. This subset was further divided into three areas during iterations by the special function ANNEAL. Residues outside of 18 Å from the centre were held rigid and were not considered; residues between 18–16 Å from the centre were tethered using a force constant of 200 kcal/(mole)*Å^2, permitting restrained movement; all residues within 16 Å (hot region) of the centre were allowed to move freely. The entire 18 Å subset of AChE was minimized using the conjugate gradient algorithm in POWELL to remove repulsive contacts between the enzyme and the inhibitor, and the TRIPOS force field consisted of only non-bonded energies: hydrogen-bonding, van der Walls, torsion and bending energy terms. The variation in distances between the Cε2 of the Trp84 and the quaternary nitrogen (N1$^+$) of the bound ligand was examined. The cut-off criterion was 8 Å radius for all interactions. The energy convergence criterion was $\pm$ 0.05 kcal mol^{-1}.

The distances used as constraints (Figure 2) were 2.7 Å for Nε2 (His440)-Oγ (Ser200); 2.5 Å for Nε2 (His440)-O of the carbonyl carbon of the carbamic moiety; 2.9, 2.9 and 3.2 Å respectively from oxyanion for Gly118, Gly119 and Ala201; 2.5 Å for Nδ1 (His440)-Oε1 (Glu327). No constraints were used for the ammonium function and for the alkyl chains of physostigmine derivatives. The RMS of each model did not exceed 0.36.

RESULTS AND DISCUSSION

The X ray structure of the complex TMTFA-*Tc*AChE, where the trifluoroketone TMTFA, **1**, is a transition state analogue, provides a useful way of organizing inhibitors **2–9** (Figure 1) in the molecular modelling tetrahedral intermediates. All the inhibitors **2–9** present similar molecular structures and rigidity. Expressly, the ester carbonyl carbon of inhibitor was positioned to form a covalent bond with the Oγ of Ser200, which mimics the nucleophilic addition of the Ser200 Oγ of the ester carbonyl group of the acetylcholine (Figure 2). The subsequent complex resembles the tetrahedral geometry of an intermediate acylating/carbamoylating step of catalysis. The quaternary nitrogen (N1$^+$) of the inhibitor was positioned within van der Waals distance (3.5 Å) of Trp84; the Oγ of Ser200 lies within hydrogen-bonding distance of His440; Glu327 is also near His440.

In Figure 2, the refined and superimposed structures **1**, **3**, **5** and **7** reveal a conformational distortion of the Trp84 residue with respect to the TMTFA-*Tc*AChE complex. When the distances are computed from the indolic Cε2

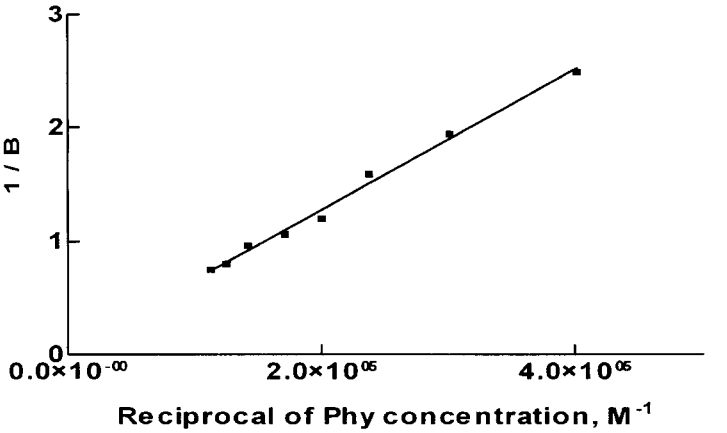

FIGURE 4 *Determination of the bimolecular rate constant for inhibition.* The values of k_i ($= k_2/K_a$) was determined from the plot of the 1/B vs. the reciprocal of Phy concentration; $[S] = 1.22 \times 10^{-1}$ M. The intercept on the ordinate axis is the reciprocal of the value of carbamylation constant k_2; the slope gives $(K_a/k_2)^*(1 + [S]/K_m)$.[10]

of the Trp84 TMTFA-AChE complex, the distortion results are smaller, 0.679 Å, for Phy (**3**), as the main interactions seem to be shared, and visually greater (1.64 Å) for the decyl-Phy (**7**). By analogy with TMTFA, the quaternary ammonium ($N1^+$) function demonstrates π-cation and van der Waals interactions with the planar aromatic face of Trp84. The primary interaction seems due to the polarizability of the approximating groups, which resolves in the characteristic non-linear relationship between the Trp84 shift and the values of k_i (Figure 5). However, we were unable to establish the precise number of interactions operating in the tetrahedral adduct which produce conformational changes down through the gorge, and perhaps, in the Cys64-Cys97 Ω loop (decyl-Phy). Analysis of the correlation between the bimolecular rate constants of inhibition, k_i, and the indolic-induced shift confirms the existence of a structural, indole-bonded catalytic mechanism (Figure 5).

A consequence of this study is the feasibility that emerges to extend this approach to the molecules of acetylcholine (ACh). In fact, the reaction of carbamates **2–9** with cholinesterases is the same basic process, which occurs when AChE catalyzes the hydrolysis of its substrate. The value of the k_{cat} constant calculated from the computational shift (0.29 Å of the Cε2 Trp84) of ACh resulted $\approx 1.9^*10^4$ s^{-1}, which is a result in good agreement with the estimated value reported in the literature.[1] However, it is conceivable that two of the assumptions made in this study, that is similar size and flexibility,

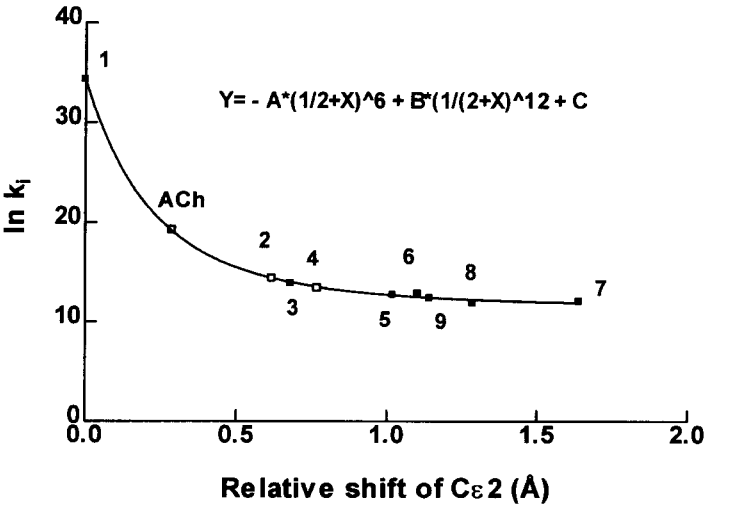

FIGURE 5 *The displacement of the Trp84 is a function of the bimolecular rate constant.* Relative shift (■) of carbon atom Cε2 of residue Trp84 and the ln of the values of the bimolecular constants, k_i ($=k_2/K_a$) for compounds **2–9**; association constant $1/K_i$ for TMTFA. (**1**). Values of parameters A, B and C for the van der Waals energy term used by the Tripos Force Field (Sybyl); the fit converged for the equation $Y = -A^*(1/(2+X)^6) + B^*(1/(2+X)) + C$ where B: 42530; A: −786.7; C: 11.6; two consecutive iterations changed the sum-of-squares by less than 0.01%; Absolute Sum of Squares: 0.348; $R^2 = 0.999$. Open symbols (□) represent the theoretical k_i values using the reported equation.

do not apply here. In fact, while there is remarkable overall similarity between the orientation of the TMTFA molecule and the physostigmine analogues as the principal interactions appear to be shared, the same considerations might not be applicable to ACh, and the model becomes oversimplified. Such transition states must be constructed with intense *ab initio*/quantum mechanical methods to properly construct the electronic and molecular properties. Furthermore, for structures, which are very different, energy minimization alone is insufficient to accurately predict protein-ligand conformations that actually occur.

The X-ray structure of the transition state analogue complex allows some considerations. Firstly, the highly geometrically converged array of TMTFA-AChE interactions describes the acylation transition state. In fact, TMTFA binds AChE about 10^{10}-fold more tightly than the ACh molecule. Secondly, the manifest overall correspondence between the alignment of the TMTFA molecule and the physostigmine analogues allows that extensive molecular dynamics or free energy pertubation calculations can be avoided. In fact, it is possible to predict realistic constants for a series of compounds

structurally related to physostigmine: 8-carbaphysostigmine (**2**, ln k_i 14.4 vs. ≈14.4,[13]), and physovenine (**4**, ln k_i 13.5 vs. ≈13.6,[14]). Other studies on AChE complexes with reversible inhibitors have shown very similar results.[15]

Regarding the mobility of Trp84, and the dynamic behaviour of the "nonregular" loop, (Cys67-Cys94), bearing Trp84, this is a area of very conflicting results.[16] In particular, molecular dynamics show the existence of a molecular device that opens to admit or remove molecules (the shutter-like back door) but site-directed mutagenesis failed to provide experimental support for the "back door" model. In addition, substantial mobility of the Ω loop, in the immediate vicinity of Trp84, even when the loop was tethered is indeed possible.[17]

However, from structural analogies to other enzymes of the lipase/esterase family, loops almost invariably assume important roles in molecular function and biological recognition.[6] This mobility, which constitutes part of the transition between the reactive and the non-reactive states, should be present also in AChE.

Acknowledgements

We are grateful to Dr. Doriano Lamba for helpful comments on various aspects of this work. We thank Dr. Silvia Sacchi for help at various stages of the modelling study and J. Clench for help in preparing the manuscript. This research was supported by the Consiglio Nazionale delle Ricerche.

References

[1] (a) T.L. Rosenberry (1975) Acetylcholineaterase. *Adv. Enzymol.*, **43**, 103–218; (b) A.R. Fersht (1985) *Enzyme Structure and Mechanism*, 2nd ed., pp. 150–152. W.H. Freeman & Company; NY.
[2] J.L. Sussman, M. Harel, F. Frolow, C. Oefner, A. Goldman, L. Toker and I. Silman (1991) *Science*, **253**, 872–879. Entry PDB 2ACE; authors: M. Harel, M.L. Raves, I. Silman & J.L. Sussman (23 June 1996).
[3] D. Pathak, K.L. Ngai and D.L. Ollis (1988) *J. Mol. Biol.*, **204**(2), 435–445; D. Pathak and D. Ollis (1990) *J. Mol. Biol.*, **214**(2), 497–525.
[4] A. Ordentlinch, D. Barak, C. Kronman, Y. Flahner, M. Leitner, Y. Segall, N. Ariel, S. Cohen, B. Velan and A. Shafferman (1993) *J. Biol. Chem.*, **268**(23), 17083–17095.
[5] A. Ordentlinch, D. Barak, C. Kronman, N. Ariel, Y. Segall, B. Velan and A. Shafferman (1995) *J. Biol. Chem.*, **270**(5), 2082–2091.
[6] J.F. Leszczynski and G.D. Rose (1986) *Science*, **234**, 849–855.
[7] (a) P. Taylor (1998) *Neurology*, **51** (1Suppl 1): S30; discussion S65–7; (b) D.S. Knopman (1998) *Geriatrics*, **53** [S31–34].
[8] M. Marta, F. Gatta and M. Pomponi (1992) *Biochim. Biophys. Acta*, **1120**(3), 262–266.
[9] G.L. Ellman, K.D. Courtney, V. Jr. Andres and M. Featherstone (1961) *Biochem. Pharmacol.*, **7**, 88–95.

[10] T. Nishioka, K. Kitamura, T. Fujita and M. Nakajima (1976) *Pestic. Biochem. Physiol.*, **6**, 320–327.
[11] M. Harel, D.M. Quinn, H.K. Nair, I. Silman and J. Sussman (1996) *J. Am. Chem. Soc.*, **118**, 2340–2346.
[12] G.S. Hammond (1955) *J. Am. Chem. Soc.*, **77**, 334.
[13] Y.L. Chen, J. Nielsen, K. Hedberg, A. Dunaiskis, S. Jones, L. Russo, J. Ives and D. Liston (1992) *J. Med. Chem.*, **35**, 1429–1434.
[14] J.R. Atack, Q.S. Yu, C. Liu, M. Brzostowska, L. Chrisey, A. Brossi, N.H. Greig, T.T. Soncrant, S.I. Rapoport and H.H. Radunz (1991) *Helv Chim Acta*, **74**, 761–766.
[15] M. Pomponi, M. Marta, S. Sacchi, A. Colella, M. Patamia, F. Gatta, F. Capone, A. Oliverio and F. Pavone (1997) *FEBS Lett.*, **409**(2), 155–160.
[16] M.K. Gilson, T.P. Straatsma, J.A. McCammon, D.R. Ripoll, C.H. Faerman, P.H. Axelsen, I. Silman and J.L. Sussman (1994) *Science*, **263**, 1276–1278; C. Kronman, A. Ordentlich, D. Barak, B. Velan and A. Shafferman (1994) *J. Biol. Chem.*, **269**(45), 27819–27822.
[17] C. Faerman, D. Ripoll, S. Bon, Y. Le Feuvre, N. Morel, J. Massoulie, J.L. Sussman and I. Silman (1996) *FEBS Lett.*, **386**(1), 65–71.
[18] D.W.J. Marquardt (1963) *Soc. Ind. Appl. Math.*, **11**, 431–441.